Taylor & Francis
Taylor & Francis Group

Plastic Solar Cells Based on Novel PPE-PPV-Copolymers

H. Hoppe
N. S. Sariciftci
Linz Institute for Organic Solar Cells (LIOS), Johannes Kepler
University, Linz, Austria

D. A. M. Egbe
Institut für Organische Chemie und Makromolekulare Chemie,
Friedrich-Schiller-Universität, Jena, Germany

D. Mühlbacher
M. Koppe
Konarka Austria, Linz, Austria

In this study plastic solar cells based on arylene-ethynylene/arylene-vinylene hybrid polymers in combination with the soluble fullerene PCBM (1-(3-methoxycarbonyl) propyl-1-phenyl [6,6]C$_{61}$) reaching 2% AM 1.5 solar power conversion efficiency at 80 mW/cm^2 are reported. The polymers used are DE105 (poly(-2,5-dioctyloxy-1, 4-phenylene-diethynylene-2,5-dioctyloxy-1,4-phenylene-vinylene-2,5-di(2′-ethyl)-hexyloxy-1,4-phenylene-vinylene)) and DE142 (poly(2,5-dioctyloxy-1,4-phenylene-ethynylene-9,10-anthracenylene-ethynylene-2,5-dioctyloxy-1,4-phenylene-vinylene-2,5-di(2′-ethyl)hexyloxy-1,4-phenylene-vinylene)), whose main difference lies in the additional anthracene group in the latter one. Comparing results from electro-chemical characterizations with IV-measurements reveals a weak dependency of the maximum open circuit voltage on the molecular HOMO level of the polymer used. A coarse grained morphology of the active layers was found responsible for limiting the photocurrent, as shown by AFM measurements.

Keywords: characterization; fullerene; morphology; novel polymer; plastic solar cell

1. INTRODUCTION

Thin film plastic solar cells based on conjugated polymer/fullerene blends are subject of increasing research interest within the past few years [1–4]. These polymer/fullerene blends or bulk heterojunctions exhibit a large interfacial area between the polymer-donor and fullerene-acceptor phases. At the materials interface a photoinduced charge transfer leads to charge separation [5], after which the charges have to travel via percolated pathways to the selective electrodes. This concept of charge generation and transport makes the bulk heterojunction approach very sensible to the underlying nanomorphology.

1.1 Solar Cell Devices Prepared from a MDMO-PPV:PCBM

(poly-[2-(3,7-dimethyloctyloxy)-5-methyloxy]-para-phenylene-vinylene: [6,6]-Phenyl C_{61} - butyric acid methyl ester) blends showed a strong dependence of the power conversion efficiency on the solvent used [6]. A solvent dependent change of the resulting nanoscale morphology has been attributed to this, which is of current research interest [7–10].

Whereas plastic solar cells based on the MDMO-PPV donor yielded power conversion efficiencies of about 2.5% [6], the use of regioregular-(poly(3-hexylthiophene-2,5-diyl) (P3HT) raised the efficiency up to 3.5% [11]. Due to the lower optical band-gap of P3HT as compared to MDMO-PPV, the photocurrent was increased considerably in case of P3HT, but the open circuit voltage stayed way below of that of MDMO-PPV based blends. Thus a further increase in power conversion efficiency due to raising the open circuit voltage is of high interest.

Earlier studies have shown the open circuit potential to depend strongly on the electron affinity (LUMO-level) of the acceptor [12] and weakly on the ionization potential (HOMO-level) of the hole conducting donor [13]. In this report we demonstrate the use of PPE-units to be an efficient way of increasing the ionization potential of the donor. This is a result of the electron-withdrawing nature of the $-C\equiv C-$moieties. Though the open circuit voltage could be kept similar or slightly increased compared to MDMO-PPV based blends, the photocurrent in PPE-PPV:PCBM devices experiences a severe limitation, which we attribute to a coarse nanomorphology, as shown by tapping mode atomic force measurements (AFM).

2. EXPERIMENTAL

2.1 Materials

The synthesis and structural characterization of the polymers **DE105** [14] and **DE142** [15] have been described elsewhere. Their chemical structure is depicted in Figure 1.
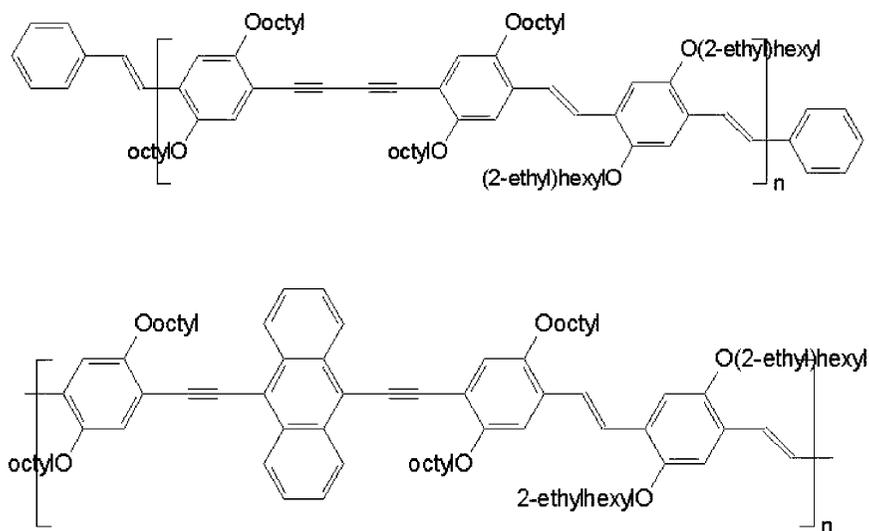
FIGURE 1 Chemical structures of the PPE-PPV copolymers DE105 (top) and DE142 (bottom).

DE105:

Poly(2, 5-dioctyl-1, 4-phenylene-diethynylene-2, 5-octyloxy-1, 4-phenylene-vinylene-2, 5-di(2′-ethyl)hexyloxy-1, 4-phenylene-vinylene-): GPC (THF): $\overline{M}_n = 24\,000$ g/mol, $\overline{M}_w = 70\,000$ g/mol, and polydispersity index = 2.9. UV-Vis (CHCl$_3$, 1.47×10^{-5} M): $\lambda_{\max}$/nm (ε/(L· mol^{-1}· cm^{-1})) 335 (23 000), 484 (91 000). Solid film (from chlorobenzene): $\lambda_{\max,abs.} = 520$ nm, $\lambda_{\max,em.} = 552$, 592 nm, $\boldsymbol{E}_g^{\mathrm{opt}} = 2.20$ eV, $\phi_{fl} = 23\%$ [14].

DE142:

Poly(2, 5-dioctyloxy-1, 4-phenylene-ethynylene-9, 10-anthracenylene-ethynylene-2, 5-dioctyloxy-1, 4-phenylene-vinylene-2, 5-di(2′-ethyl)-hexyloxy-1, 4-phenylene-vinylene): (GPC (THF): $\overline{M}_w = 36\,000$ g/mol, $\overline{M}_n = 21\,000$ g/mol, $\overline{M}_z = 55\,000$ g/mol, $M_p = 32\,000$ g/mol, polydispersity index = 1.7. UV-Vis (CHCl$_3$, 9.0×10^{-6} M): $\lambda_{\max}$/nm (ε/(L·mol^{-1} · cm^{-1})) 282 (60 160), 322 (30 000), 540 (83 100). Solid film (from chlorobenzene): $\lambda_{\max,abs.} = 575$ nm, $\lambda_{\max,em.} = 620$ nm, $\boldsymbol{E}_g^{\mathrm{opt}} = 1.90$ eV, $\phi_{fl} = 12\%$ [15].

Poly[2-(3,7-dimethyloctyloxy)-5-methoxy-*p*-phenylene-vinylene] (MDMO-PPV) obtained from Covion (Germany) was also investigated for the purpose of comparison. Regio-regular P3HT (poly(3-hexylthiophene-2,5-diyl) was purchased from Rieke Metals Inc. (Nebraska, USA). PCBM ((1-(3-methoxycarbonyl) propyl-1-phenyl [6,6]C$_{61}$) was purchased from J. C. Hummelen (Univ. of Groningen, The Netherlands).

We used poly[3,4-(ethylenedioxy) thiophene] : poly(styrene sulfonate) (PEDOT:PSS, Baytron PH) from Bayer (Leverkusen, Germany) as anode. As transparent conducting substrates we used ITO glass, purchased from Merck (Darmstadt, Germany). The cathode materials used were evaporated Aluminium in combination with a thin LiF interlayer.

2.2 Device Preparation

After etching a part of the ITO glass to allow selective contacting of the back electrode (cathode), films of PEDOT:PSS were either spin cast at 1500 rpm or doctor bladed from aqueous solution onto the ITO substrate. Next, the photoactive layer was spin cast at 1500 rpm or doctor bladed from chlorobenzene solution. Finally the top aluminum electrode (with or without LiF) was evaporated in a vacuum chamber. Cell areas varied between 10–20 mm^2. A schematic of the device structure is shown in Figure 2.

2.3 Characterization Methods

The solar cell devices were characterized by current-voltage (I–V) measurements. To determine the solar power conversion efficiency, I–V-characteristics under 80 mW/cm^2 white light illumination from a solar simulator were taken.

To determine the HOMO-LUMO levels of the materials, cyclic voltammetry (CV) and electrochemical voltage spectroscopy (EVS)
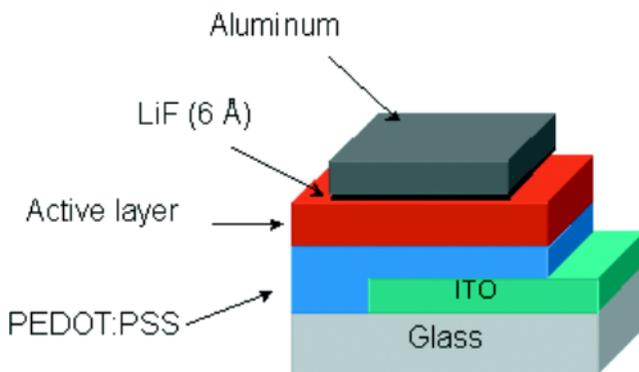
FIGURE 2 Schematic structure of plastic solar cells. The active layer consists of a blend of a conjugated polymer and the fullerene PCBM.

measurements were performed. The electrochemical measurements were carried out at room temperature in a glove-box using a Jaissle potentiostat computer controlled with SCADA software. The supporting electrolyte was $0.1\,M$ $(C_4H_9)_4N^+PF_6^-$ in acetonitrile, the working and the counter electrode were platinum foils. The reference electrode (RE) was a silver wire coated with AgCl.

The EVS method gives basically the change of the injected charges with the electrode potential $\Delta Q/\Delta E$, which can be plotted vs. E and can be interpreted as an infinitesimally slow cyclic voltammogram. Spectral photocurrent was recorded under illumination of a monochromatized Xenon-lamp with a typical illumination density of $5\text{--}10\,\mu W$. The incident beam was chopped with a mechanical chopper, the photocurrent was detected with a lock-in-amplifier. The Xe-lamp spectrum was measured with a calibrated Si-diode.

The morphology and film thickness of the active layers was investigated by tapping mode AFM measurements, using a Dimension 3100 system (Digital Instruments, Santa Barbara, CA).

3. RESULTS AND DISCUSSION

The structure of the PPE-PPV copolymers used is depicted in Figure 1, whereas their synthesis is described elsewhere [14,15]. DE105 is a copolymer of a PPE-unit containing two consecutive triple bonds and one PPV-unit. In contrast, the DE142 copolymer includes an electron rich anthracene-unit between the triple bonds, leading to a red shift of the absorption edge by roughly $50\,nm$ as compared to DE105. These compounds are thermo stable up to around $330\text{--}350°C$, where approximately 5% weight-loss was observed.

Solar cell devices were prepared with a structure depicted in Figure 2. The devices were characterized by current voltage (IV) measurements under a simulated solar spectrum of $80\,mW/cm^2$ and by spectral photocurrent measurements.

To determine the molecular energy levels, cyclic voltammetry (CV) and electrochemical voltage spectroscopy (EVS) were applied. The electrochemical results for DE105, DE142, MDMO-PPV and regioregular P3HT are summarized in Table 1 together with the highest achieved open circuit voltages. There is a weak relation between the polymer HOMO level and the maximum observed photovoltage.

The highest power conversion efficiency obtained with polymer DE142 has been attained with devices prepared by the doctor blade technique. The best devices showed power conversion efficiencies about 2% at $80\,mW/cm^2$ solar irradiation, with a short circuit current of $3\,mA/cm^2$, open circuit voltage of $820\,mV$ and filling factor of 64%.

TABLE 1 Comparison of Molecular Energy Levels Determined by Electro-chemistry and Maximum Open Circuit Voltages Obtained on the Solar Cell devices. There is a Weak Correlation between the Polymer HOMO-level and the Maximum Open Circuit Voltage

| Compound	LUMO/eV	HOMO/eV	E_g/eV	V_{OCmax}/V
DE105	-3.25	-5.51	2.26	~ 0.90
DE142	-3.31	-5.36	2.05	~ 0.85
MDMO-PPV	-3	-5.26	2.26	~ 0.84
P3HT	-2.9	-5.1	2.2	~ 0.58

In Figure 3 some IV-curves of these devices measured under illumination are presented. Here the thickness of the active layer was varied by the coating conditions and an increase in the photocurrent for the thicker layer (195 ± 5 nm) as compared to the thinner one (145 ± 5 nm) could be achieved. However, though the optical band gap of the polymer DE142 is lower than that of MDMO-PPV, the photocurrents are
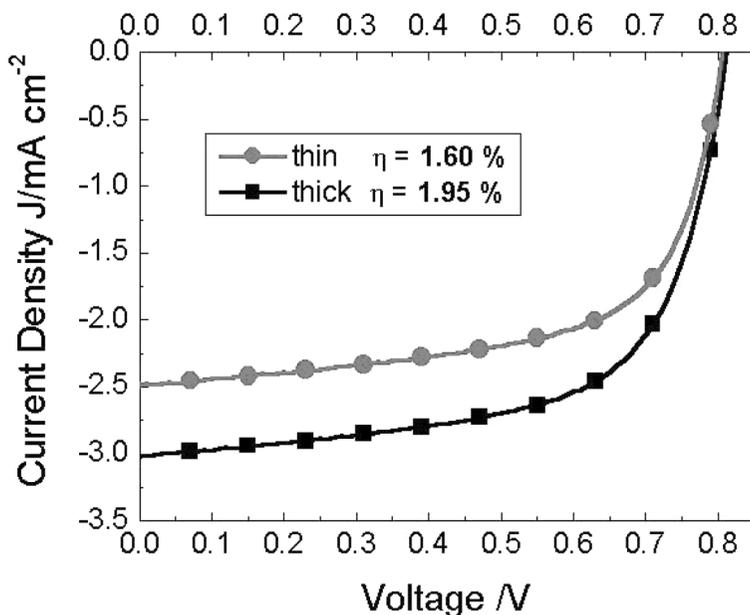
FIGURE 3 Current-voltage characteristics of investigated devices based on DE142:PCBM 1:2 under $80\,mW/cm^2$ solar simulator illumination. The film thickness was determined by AFM to be ca. 145 ± 5 nm for the thinner and 195 ± 5 nm for the thicker active layer.
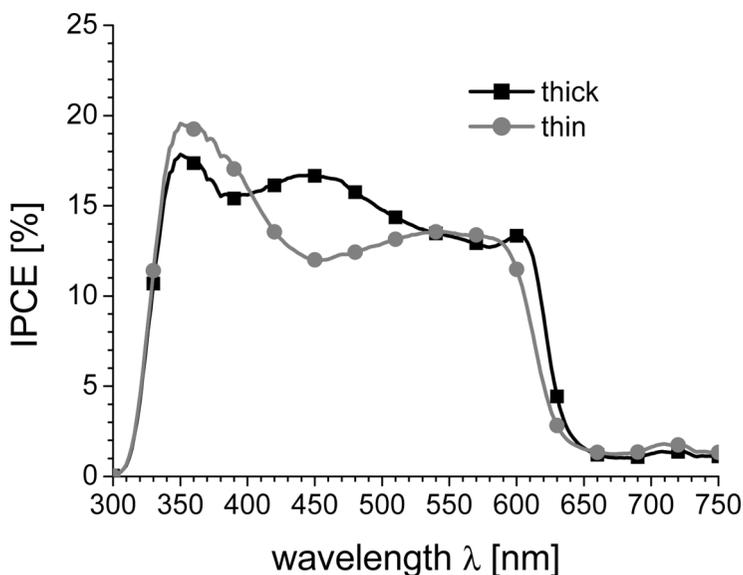
FIGURE 4 Incident photon to collected electron (IPCE) spectra of the two doctor bladed devices based on DE 142:PCBM 1:2 blends. The relatively low absolute IPCE values reflect the limited photocurrent.
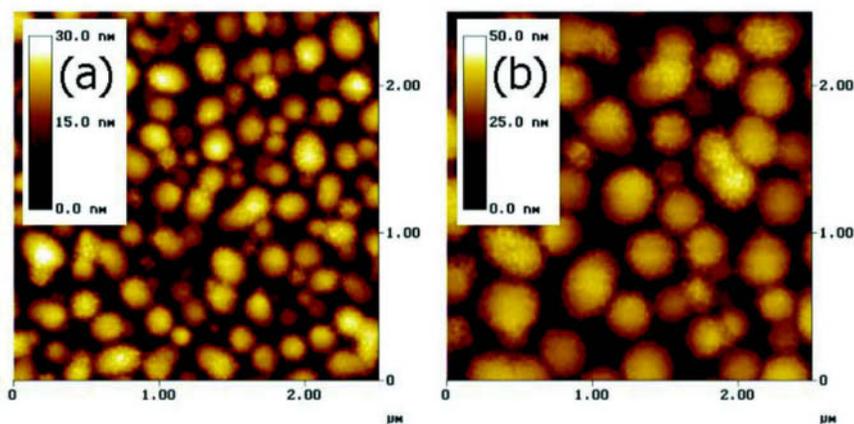
FIGURE 5 Tapping mode scanning probe microscopy performed on the active layers of the DE142:PCBM 1:2 devices under investigation here. The topography of the thinner (a) and the thicker (b) device are shown, and a considerable increase in feature size for the thicker device is observed. The films were produced by doctor blading.

smaller. This is also reflected by the spectral photocurrent measurements, demonstrating the low external quantum yield (compare Fig. 4). The origin of this was attributed by tapping AFM measurements to a rather coarse grained nanomorphology. The scale of phase separation of the thicker device is comparable with blends of MDMO-PPV:PCBM cast from toluene solvent [10] (Fig. 5). Therefore it is expected that not all photoexcitations will lead to separated charge carriers and thus resulting photocurrent. Since high filling factors are an indication for good charge transport properties, we expect the low photocurrents to be due to limited charge generation rather than transport losses.

4. CONCLUSION

Plastic solar cells prepared from novel PPE-PPV hybrid copolymers and PCBM show promising power conversion efficiencies of about 2%. A weak correlation between the molecular HOMO level of the donor and the maximum achievable open circuit voltage is found. AFM measurements show a large-scale phase separation in the photoactive layer. This is in agreement with the low external quantum efficiencies determined for these devices, leading to comparably small photocurrents. Further work will be dedicated to the morphology optimization.

REFERENCES

[1] Brabec, C. J., Sariciftci, N. S., & Hummelen, J. C. (2001). Plastic Solar Cells. *Adv. Funct. Mater.*, *11*, 15.
[2] Nelson, J. (2002). Organic photovoltaic films. *Curr. Opin. Solid State Mater. Sci.*, *6*, 87.
[3] In (2003) *Organic Photovoltaics: Concepts and Realization*, Brabec, C. J., Dyakonov, V., Parisi, J., & Sariciftci, N. S. (Eds.), Berlin, Vol. 60.
[4] Hoppe, H. & Sariciftci, N. S. (2004). Organic solar cells: an overview, *Journal of Materials Research*, *19*, 1924.
[5] Sariciftci, N. S., Smilowitz, L., Heeger, A. J., & Wudl, F. (1992). Photoinduced electron transfer from a conducting polymer to buckminsterfullerene. *Science*, *258*, 1474.
[6] Shaheen, S. E., Brabec, C. J., Sariciftci, N. S., Padinger, F., Fromherz, T., & Hummelen, J. C. (2001). 2.5% efficient organic plastic solar cells. *Appl. Phys. Lett.*, *78*, 841.
[7] Martens, T., D'Haen, J., Munters, T., Beelen, Z., Goris, L., Manca, J., D'Olieslaeger, M., Vanderzande, D., Schepper, L. D., & Andriessen, R. (2003). Disclosure of the nanostructure of MDMO-PPV:PCBM bulk heterojunction organic solar cells by a combination of SPM and TEM. *Synth. Met.*, *138*, 243.
[8] Martens, T., Beelen, Z., D'Haen, J., Munters, T., Goris, L., Manca, J., D'Olieslaeger, M., Vanderzande, D., Schepper, L. D., & Andriessen, R. (2003) "Morphology of

MDMO-PPV:PCBM bulk hetero-junction organic solar cells studied by AFM, KFM and TEM," presented at the Proceedings of the SPIE The International Society for Optical Engineering, San Diego, CA. (SPIE The International Society for Optical Engineering), p. 40.

[9] Yang, X., van Duren, J. K. J., Janssen, R. A. J., Michels, M. A. J., & Loos, J. (2004). Morphology and Thermal Stability of the Active Layer in Poly(*p*-phenylenevinylene)/Methanofullerene Plastic Photovoltaic Devices. *Macromolecules*, *37*, 2151.

[10] Hoppe, H., Niggemann, M., Winder, C., Kraut, J., Hiesgen, R., Hinsch, A., Meissner, D., & Sariciftci, N. S. (2004). Nanoscale morphology of conjugated polymer/fullerene based bulk-heterojunction solar cells. *Adv. Funct. Mater.*, *14*, 1005.

[11] Padinger, F., Rittberger, R. S., & Sariciftci, N. S. (2003). Effects of Postproduction Treatment on Plastic Solar Cells. *Adv. Funct. Mater.*, *13*, 1.

[12] Brabec, C. J., Cravino, A., Meissner, D., Sariciftci, N. S., Fromherz, T., Rispens, M. T., Sanchez, L., & Hummelen, J. C. (2001). Origin of the Open Circuit Voltage of Plastic Solar Cells. *Adv. Funct. Mater.*, *11*, 374.

[13] Kim, H., Jin, S.-H., Suh, H., & Lee, K. (2003). "Origin of the open circuit voltage in conjugated polymer-fullerene photovoltaic cells," presented at the Proceedings of the SPIE The International Society for Optical Engineering, San Diego, CA.

[14] Egbe, D. A. M., Bader, C., Nowotny, J., & Klemm, E. (2003). Presented at the Proceedings of the SPIE The International Society for Optical Engineering, San Diego, CA, p. 79.

[15] Hoppe, H., Egbe, D. A. M., Mühlbacher, D., & Sariciftci, N. S. (2004). Photovoltaic action of conjugated polymer/fullerene bulk heterojunction solar cells using novel PPE-PPV-copolymers. *J. Mater. Chem.*, 3462.